Cancer Research

hnRNP A2/B1 Modulates Epithelial-Mesenchymal Transition in Lung Cancer Cell Lines

Jordi Tauler[1], Enrique Zudaire[2], Huaitian Liu[3], Joanna Shih[4], and James L. Mulshine[1]

Abstract

Heterogeneous nuclear ribonucleoprotein A2/B1 (hnRNP A2/B1) has been reported to be overexpressed in lung cancer and in other cancers such as breast, pancreas, and liver. However, a mechanism linking hnRNP A2/B1 overexpression and progression to cancer has not yet been definitively established. To elucidate this mechanism, we have silenced hnRNPA2/B1 mRNA in non–small-cell lung cancer cell lines A549, H1703, and H358. These cell lines present different levels of expression of epithelial-to-mesenchymal transition (EMT) markers such as E-cadherin, fibronectin, and vimentin. Microarray expression analysis was performed to evaluate the effect of silencing hnRNP A2/B1 in A549 cells. We identified a list of target genes, affected by silencing of hnRNP A2/B1, that are involved in regulation of migration, proliferation, survival, and apoptosis. Silencing hnRNP A2/B1 induced formation of cell clusters and increased proliferation. In the anchorage-independent assay, silencing hnRNP A2/B1 increased colony formation by 794% in A549 and 174% in H1703 compared with a 25% increase in proliferation, in both cell lines, in a two-dimensional proliferation assay. Silencing hnRNP A2/B1 decreased migration in intermediate cell line A549 and mesenchymal cell line H1703; however, no changes in proliferation were observed in epithelial cell line H358. Silencing hnRNP A2/B1 in A549 and H1703 cells correlated with an increase of E-cadherin expression and downregulation of the E-cadherin inhibitors Twist1 and Snai1. These data suggest that expression of hnRNP A2/B1 may play a role in EMT, in nonepithelial lung cancer cell lines A549 and H1703, through the regulation of E-cadherin expression. *Cancer Res; 70(18); 7137–47. ©2010 AACR.*

Introduction

Heteregeneous nuclear ribonucleoprotein A2/B1 (hnRNP A2/B1) is a member of the hnRNP family of proteins. The hnRNPs are a complex group of RNA-binding proteins that play a key role in mRNA processing and telomere biogenesis (1–4). hnRNP A2/B1 overexpression has been described in many cancers, including breast, pancreas, liver, and gastrointestinal cell lines (5–8). Recent reports have described a critical role of hnRNP A2/B1 in the regulation of fundamental biology especially related to cancer, such as migration (9) and aerobic glycolysis (10). We have previously reported that hnRNP A2/B1 is a marker for early lung cancer (11–15). Overexpression of hnRNP A2/B1 in exfoliated bronchial epithelial cells of archival sputum samples correlated with eventual development of lung cancer (16). High levels of hnRNP A2/B1 expression also colocalized with areas of genetic injury, as assessed by microsatellite instability and loss of heterozygosity (17). hnRNP A2/B1 has been consistently reported as an informative biomarker for lung cancer screening using a variety of analytic approaches, including expression studies and proteomic analysis (7, 8, 18, 19). We have also previously reported that hnRNP A2/B1 expression is tightly controlled during lung development (20). A recent article has shown the impact of cell density on hnRNP A2/B1 expression, reporting that mouse lung cell lines E9 and E10 both showed increase of hnRNP A2/B1 protein related to proliferation. At confluency, the nontumorigenic E10 cell line downregulated hnRNP A2/B1 mRNA production, whereas the tumorigenic E9 cell line showed an increase of total hnRNP A2/B1 production (21).

However, the contribution of hnRNP A2/B1 to the carcinogenic process is still poorly understood. Some reports have used silencing tools in different cancer cell lines to study the function of hnRNP A2/B1 (22–24). Silencing hnRNP A2/B1 in combination with hnRNP A1 reduced cell growth by inducing cell death in cancer cell lines (22). Silencing hnRNP A2/B1 alone in squamous carcinoma cell line, Colo16, regulated genes involved in cell cycle and proliferation; however, it had a modest effect in Colo16 proliferation (23, 24).

Recent evidence is showing a prominent role of hnRNP A2/B1 in fundamental biological functions such as regulation of cell metabolism (10), migration and invasion (9, 25, 26), proliferation (22–24), and cellular response to mitochondrial

Authors' Affiliations: [1]Laboratory of Lung Cancer Biology, Section of Medical Oncology, Rush University Medical Center, Chicago, Illinois; [2]NCI Angiogenesis Core Facility, National Cancer Institute, NIH, Advanced Technology Center, Gaithersburg, Maryland; [3]Science Applications International Corporation, Rockville, Maryland; and [4]Biometric Research Branch, Division on Cancer Treatment and Diagnosis, National Cancer Institute, NIH, Bethesda, Maryland

Note: Supplementary data for this article are available at Cancer Research Online (http://cancerres.aacrjournals.org/).

Corresponding Author: Jordi Tauler, Rush University Medical Center, Room 1413, Jelke Building, 1750 West Harrison Street, Chicago, IL 60612. Phone: 312-942-3595; Fax: 312-563-3377; E-mail: Jordi_Tauler@rush.edu.

doi: 10.1158/0008-5472.CAN-10-0860

stress (26). Moreover, hnRNP A2/B1 activation of invasion phenotype involves different mechanisms including activation of the CXCL-12/CXCR4 axis (25), alternative splicing of TP53INP2 (9), and activation of invasive behavior, after depletion of mitochondrial DNA, through hnRNP A2/B1–mediated cooperative effect of NF-κB, NFAT, CREB, and C/EBPδ (26). Interestingly, it has been reported that depletion of mitochondrial DNA in cancer cells promotes epithelial-mesenchymal transition (EMT; ref. 27). Moreover, it has also been proposed that changes in morphology, invasion, and metastasis potential could be the result of EMT (28, 29).

To investigate how the overexpression of hnRNP A2/B1 affects this important functional biology in lung cancer, we modified the expression of hnRNP A2/B1. Because hnRNP A2/B1 is playing a role in the regulation of migration activity, we used lung cancer cell lines with different levels of EMT phenotype markers such as mesenchymal H1703, intermediate A549, and epithelial H358 (30). We have, for the first time, noted significant changes in proliferation and migration in nonepithelial H1703 and A549 lung cancer cell lines associated with changes in cell morphology, suggesting that hnRNP A2/B1 may be an important regulator of EMT and could provide a mechanistic link between hnRNP A2/B1 overexpression and tumor progression.

Materials and Methods

Cell cultures

Cell lines used in this study include A549, H1703, and H358 non–small cell lung cancer (NSCLC) cell lines obtained from the American Type Culture Collection. These cell lines present different EMT phenotypes as determined by the expression of EMT markers. H1703 has been classified as mesenchymal, whereas A549 and H358 display a more epithelial phenotype (30). Cells were maintained in RPMI 1640 supplemented with 5% fetal bovine serum (FBS; Hyclone), in 95% air and 5% CO_2 at 37°C. Cells were counted and seeded at 1×10^6 per flask in a new T75 flask at every passage.

siRNA expression vectors

Oligonucleotides for the siRNA vectors were designed with the Web-based software provided by Oligoengine. Sequences for the three different oligonucleotides were as follows: siA, ACGTGCTGTAGCAAGAGAG; siD, CCAGGGGCTCATGTAACTG; siE, TTTTGGAGGTAGCCCCGGT. siRNA oligonucleotides from Oligoengine were ligated and cloned in pSuper.neo (Oligoengine) vector following the manufacturer's protocol. Cells were transfected with Fugene 6 (Roche) following the manufacturer's protocol and selected with 800 μg/mL of G418 (Hyclone). After selection, transfected cells were maintained in medium supplemented with G418 at 300 μg/mL (Hyclone). We have stably transfected NSCLC A549, H1703, and H358 cell lines with three different constructs (siA, siD, and siE) and empty vector (EV) as a control.

cDNA expression vectors

cDNA expression vector for hnRNP A2/B1, based on TrueORF cDNA clones system, was acquired from Origene. Cell line A549 was transfected with Fugene 6 (Roche), and transfected cells were selected using the protocol described above. Cell lines A549 EV-TC (Empty Vector True Clone) and A549 A2B1rec (expressing hnRNP A2/B1) were obtained.

Microarray data generation

A549 EV and A549 siA cells were seeded at 1.5×10^6 in a T75 flask. At 60 hours postseeding, total RNA was extracted using RNeasy mini-kit (Quiagen). First-strand cDNA, double-strand cDNA, and cRNA were synthesized and processed according to the manufacturer's protocol (Affymetrix). Microarray study was performed using Affymetrix HG U133 Plus 2.0. Protocol for data analysis can be found in Supplementary Materials (Supplementary Microarray Data Analysis and Legends, and Supplementary Figs. S1–3).

Real-time PCR

For real-time PCR of samples depicted in Figs. 1A,B, 4A,B, and 5D, cells were seeded at 2×10^6 in a T75 flask. For real-time PCR for samples in Fig. 5A to C, cells were seeded at 0.7×10^6 in a T25 flask. Total RNA was extracted after 24 hours postseeding (Figs. 1A,B, 4A,B, and 5D) and at 0, 2, 4, and 6 hours (Figs. 5A–C) with RNeasy Mini-kit (Qiagen). Total RNA (0.8–2 μg) for each analyzed sample was reverse transcribed in a final volume of 25 μL using SuperScript First-Strand Synthesis kit (Invitrogen). Quantitative real-time PCR reaction was performed in a final volume of 25 μL containing 2 μL of cDNA (1:10 dilution) and 400 nmol/L of primers and SybrGreen PCR master mix (Applied Biosystems), and run in an Opticon Cycler (MJ Research) and in a 7300 Cycler (Applied Biosystems). All samples were amplified in triplicate using the following cycle scheme: 50°C for 2 minutes; 95°C for 10 minutes; and 45 cycles of 95°C for 30 seconds, 60°C for 30 seconds. Final mRNA levels were normalized to 18S rRNA levels. All results are plotted as columns (mean) and bars (SD), calculated with 7300 Real-Time PCR System SD Software (Applied Biosystems). Primer sequences can be found in Supplementary Table S1.

Western blotting

Cells were seeded at 3×10^5 per well in a six-well plate for 24 hours. For each cell line, three wells were used. For cell density experiments, cells were seeded at described densities in T75 flask. To obtain whole-cell extracts, cells were washed with cold 1× PBS (Bio-Rad), scrapped from a six-well plate or T75 flask, and disrupted with 150 μL of lysis buffer: 100 mmol/L Tris-HCl (pH 7.4), 150 mmol/L NaCl, 1% Triton X-100 (Bio-Rad) supplemented with 1× HALT protease inhibitor cocktail (Pierce), and 1× HALT phosphatase inhibitor cocktail (Pierce). After 30 minutes of incubation on ice, whole-cell extracts were cleared by centrifugation. Protein concentration was calculated with the BCA method (Pierce), and 10 to 60 μg of total protein were loaded on ReadyGel 4% to 15% Tris-HCl from Bio-Rad. Western

blotting was performed following standard conditions with primary antibody: diluted 1:1,000 for hnRNP A2/B1 (sc-10035; Santa Cruz), 1:1,000 for actin (sc1616; Santa Cruz), 1:1,000 for E-cadherin (3195; Cell Signaling), 1:250 for Snai1 (3879; Cell Signaling), 1:500 for fibronectin (sc-9068; Santa Cruz), and detected with ECL Plus Western blot detection system (GE Healthcare). Images were analyzed using a FluorChem SP system (Alphainnotech). Actin was used as a loading control. Relative optical density was calculated using ImageJ free software (31).

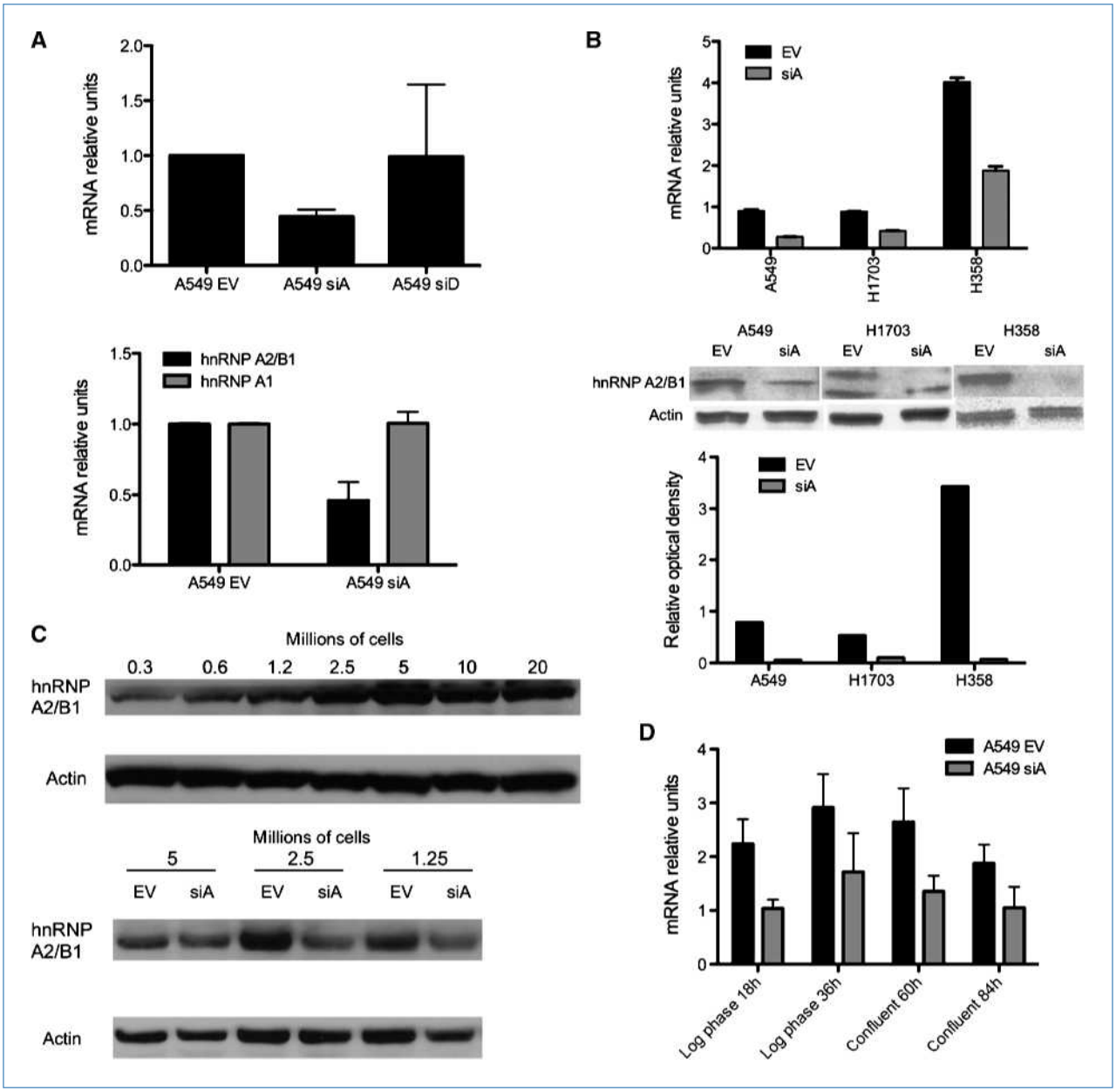

Figure 1. Validation of silenced hnRNP A2/B1. A, top, comparison of siRNA efficiency of siA and siD constructs in A549-transfected cells. Bottom, expression of hnRNP A2/B1 and hnRNP A1 in A549 after silencing hnRNP A2/B1. B, top, expression of hnRNP A2/B1 in transfected cells with a siA silencing construct. Middle, hnRNP A2/B1 silencing in whole-cell extracts of A549 siA, H1703 siA, and H358 siA by Western blot. Bottom, relative optical density of hnRNP A2/B1 normalized to actin. C, top, effect of cell density on expression of hnRNP A2/B1 in A549 cells seeded at increasing density. Whole-cell extracts were obtained after 60 hours postseeding. Bottom, silencing efficiency is affected by cell density in A549 cells. A549 EV and A549 siA cells were seeded at increasing cell density. Whole-cell extracts were obtained after 72 hours postseeding. D, selection of optimal conditions for hnRNP A2/B1 silencing to be used in microarray analysis. RNA from A549 EV and A549 siA was extracted in cells growing in exponential phase at 18 and 36 hours, and confluent cells at 60 and 84 hours postseeding. Experiments were repeated three times.

Growth assay and anchorage-independent growth assay

Growth was determined using CellTiter 96 AQueous One Solution Cell Proliferation Assay (Promega) following the manufacturer's protocol. Experiments were performed in 96-well plates using RPMI 1640 containing 5% FBS. A549 EV and A549 siA cells were seeded from 2,500 and 10,000 per well. H1703 EV and H1703 siA cells were seeded at 20,000 and 30,000 per well. Assay reading was performed on a 96-well plate reader (FLUOstar Optima, BMG Labtech). The anchorage-independent growth of A549 EV, A549 siA, H1703 EV, and H1703 siA cells was examined by soft agar clonogenic assay. Briefly, 5,000 cells were resuspended in 1.5 mL of the culture medium containing 10% FBS and 0.3% agarose and plated in six-well plates with 1.5 mL of presolidified culture media in 0.5% agar containing 10% FBS. Plates were incubated at 37°C for 4 weeks, and colonies larger than 0.1 mm in diameter were counted. All results are plotted as columns (mean) and bars (SD).

Migration assay

Chemotaxis was assayed in 8-μm pore, 96-well ChempTx plates (Neuroprobe). Cells were resuspended at 100,000/mL and seeded at 35 μL/well (3,500 cells per well). Cells were placed in the upper chambers, and the lower chambers were filled with RPMI–10% FBS. After a 4-hour migration period at 37°C, nonmigrating cells were wiped off the top surface of the membrane. Membranes were fixed and stained with Hema3 (Biochemical Sciences), and the cells trapped in the pores of the membrane were counted.

Immunofluorescence

Cells were seeded in Lab-Tek II four-well glass chamber slides (Nunc) at 60,000 per chamber. Cells were incubated for 24 hours at 37°C, fixed with formalin (Fisher Scientific) for 10 minutes at room temperature, washed with PBS and permeabilized with 100% ice-cold methanol at −20°C for 10 minutes, and washed with PBS and blocked with PBS containing 5% of normal goat serum and 0.1% Triton X-100. Cells were incubated with primary antibody to E-cadherin (1:100) overnight at 4°C, washed with PBS, and then incubated with secondary antibody conjugated with TRITC (1:100; Pierce) for 1.5 hours. After washing, coverslips were attached to glass slides with Vectashield mounting medium containing 4′,6-diamidino-2-phenylindole (Vector Laboratories). Cells were imaged using a fluorescence microscope (Olympus BX41, Olympus America), and images were processed using Spot Advanced v.4.6 software (Diagnostic Instruments).

Results

Silencing hnRNP A2/B1 in lung cancer cell lines

Although siA and siD sequences are separated by only 12 nucleotides, the silencing effects observed with these oligonucleotides are very different. siD was able to show a moderate but not consistent silencing of hnRNP A2/B1. siE had no effect in silencing hnRNP A2/B1 (data not shown). siA was the only construct that showed consistent and significant silencing of hnRNP A2/B1 compared with EV (Fig. 1A). Because previous observations have suggested a cooperative interaction between hnRNP A2/B1 and hnRNP A1, we evaluated expression of hnRNP A1 after silencing hnRNP A2/B1. We did not observe changes in hnRNP A1 mRNA expression (Fig. 1A). Downregulation of hnRNP A2/B1 at the mRNA and protein levels was confirmed in A549, H1703, and H358 cell lines (Fig. 1B).

We and others have reported that cell density affects hnRNP A2/B1 expression (11, 21) in several lung cancer cell lines. Cell density at seeding affects hnRNP A2/B1 expression and predictably determines the timing of hnRNP A2/B1 peak of expression in A549 cell line (Fig. 1C). We examined the influence of cell density in silencing of hnRNP A2/B1 in A549. At 72 hours postseeding, A549 EV cells seeded at 1.25×10^6 per flask were 90% confluent, and cells seeded at 2.5×10^6 per flask were at confluency. Maximal differences in hnRNP A2/B1 protein levels between A549 EV and A549 siA cells were detected just as cells reached confluency (Fig. 1C).

Effects of hnRNP A2/B1 silencing on gene expression in A549 cell line

We extracted RNA from A549 EV and siA cells at four different time points to evaluate conditions for optimal silencing. At 60 hours postseeding, expression of hnRNP A2/B1 mRNA in A549 EV was still near maximum. At this time point, mRNA levels of hnRNP A2/B1 in A549 EV compared with A549 siA showed an efficiency of silencing around 50% (Fig. 1D). Microarray analysis was performed under these conditions. We obtained a list of 173 differentially expressed genes between A549 EV and A549 siA cells (see list in Supplementary Materials; Supplementary Table S2). Network association analysis resulted in these 173 genes being categorized into nine clusters according to their known functional relationship as described in the Ingenuity Pathway Knowledge Base (Table 1). Different significant biological functions were revealed by this method as reported in Supplementary Table S3. The most relevant functions affected by silencing hnRNP A2/B1 in A549 cell line were cellular movement, cellular development, amino acid metabolism, and cell death. Interestingly, pathways central to embryonic development also were found in the nine clusters. These results, in combination with 64 genes involved in cancer (see list Supplementary Materials; Supplementary Table S4), are consistent with a role for hnRNP A2/B1 in cancer that could represent a modification of developmental programs as we have reported previously (20). Moreover, we have validated the microarray results by real-time PCR, using 27 of the 173 genes, and reported that 25 (93%) show similar results after microarray and real-time PCR analyses (see table and figure in Supplementary Materials, Supplementary Fig. S4).

Silencing hnRNP A2/B1 affects morphology of nonepithelial cell lines

After 72 hours postseeding, A549 EV cells consistently presented a more homogeneous cell shape and size, and are completely confluent. A549 siA cells did not cover the whole surface of the flask and revealed a pattern of high-density

Table 1. Results from microarray study

ID	Molecules in network	Score	Focus molecules	Top functions
1	***CACNB2***, collagen(s), ***CP, ELOVL2, ENTPD1***, ERK, Fascin, ***FHL1, FN1, FSCN1, GDF15, GJA1, GJC1, GSN, H19***, *hCG*, ***IGFBP2, INHBB, LPAR1***, Nfat, ***NPR3, NTS, PAPPA***, *Pdgf, PDGF BB*, ***PDGFC, PGM2L1***, Pkc(s), *PLC*, ***PLCB4***, *Rac*, ***S1PR3, SLC1A1, TGFB2, VCAN***	44	25	Cancer, amino acid metabolism, small-molecule biochemistry
2	***ABCB1***, Akt, ***AKT3***, *Ap1*, ***CD24, DNER, EDAR, ERBB3, HIPK2***, *IFNβ, IL1, IL6ST*, insulin, Jnk, *LDL*, ***LEPR***, Mapk, ***MFHAS1***, NF-κB (complex), ***NR2F1, OAS1***, *P38 MAPK*, ***PCSK9***, *PI3K*, ***PPARGC1A, PRSS1, PRSS3, SERPINA1, TFPI2, TLE1, TNS3***, Trypsin, ***UTRN***, Vegf, ***WNT4***	40	22	Cancer, cell death, neurologic disease
3	Actin, ***CA12***, *CACNA1A*, caspase, *Ck2, CPLX1*, ***CUX1***, *DSG1, DSG3*, F-actin, *FSH*, ***GPRC5B, HNRNPA2B1***, *HOXB8*, ***JUP, MEIS2***, *MIRN346*, ***NOVA1, NR3C2, NRCAM***, *NRXN1*, ***NTRK3, PBX1***, Pka, *PKN2, PSEN1, RAB8B, S100A13, SLC14A2*, ***SNAP25***, Snare, ***SYT1***, *SYT3*, ***VIL1***, *ZDHHC17*	24	15	Nervous system development and function, small-molecule biochemistry, behavior
4	***ATG12***, *CASP3, CDC37*, ***CIDEC***, corticosterone, ***CPS1, CPVL***, *DSP*, ***HYAL1***, hyaluronic acid, ***KCTD12***, L-dopa, *MAP3K3*, ***MMD, MSRB3***, *MYCN*, ***MYO1A***, *PKN2, PPARA, PRKCZ, PSEN1, RAF1*, ***SFI1, SLC1A2, SRPX***, *TGFA, TNF, TRAF6*, ***UBXN10***, *VCP, VIP*, ***WWOX***, *YWHAG, YWHAZ, ZFP36*	22	14	Cell death, cellular development, hair and skin development and function
5	***ACSL5***, *ALB, AMBP, ATG3, CD302, CEBPA*, ***CLDN1, CRB1, CRIP1, ELOVL7***, *HIST2H4A, HNF1A*, HNF4α dimer, *HNF4A*, ***HNMT***, *HPX, LEF1, LEP, LGALS3, LUC7L2, MIRN31*, ***MOCOS***, *PDX1*, ***PEG10***, *PPARA, PZP*, ***SFRS1***, *SREBF1*, ***SRI, SSFA2***, *TCF7L2, TRAF2*, ***TRIM31***, *UBE2I, YWHAG*	20	13	Lipid metabolism, small-molecule biochemistry, carbohydrate metabolism
6	***ADORA2B***, aryl sulfotransferase, *BDNF*, β-estradiol, *CEBPA, CHST7*, cyclic AMP, *DLG4, DRD1, GABAR-A*, ***GABRA5***, *GABRB1*, ***GABRB2***, *GABRB3, GABRG2, GABRG3, HTR1A, MIRN196A1, MIRN196A2, MIRN196B*, ***PDE1A, PKIB***, potassium, pregnenolone, *RAF1, SET*, ***SETBP1, SLC6A14, STK32B***, sulfotransferase, ***SULT1A1, SULT1A2, SULT1A3, TOX3***	20	13	Genetic disorder, nutritional disease, psychological disorders
7	***ALX1***, *ANXA5*, ***ATRX***, calpain, *CBX5, CDKN1A, CEBPA, CTNNBIP1*, D-glucose, ***DCLK1, DSE***, *EP300*, ***EYA4, HMGB3***, *KLF6*, ***KRT4***, *LEF1, LEP, MBP, MIRN124, MIRN106B, NR3C1, PDX1, PPARA, PRKCZ, PSMD4*, ***RASSF8, RIMKLB, SCN9A, ST8SIA4, STOM***, *TGFA*, ***TM4SF18***, *TP53INP1, YY1*	20	13	Gene expression, organ development, carbohydrate metabolism
8	***ABCC6***, *ANXA2, AXIN1, BDNF*, ***CADM1***, *CEBPA, CREB1*, cyclic AMP, *HRAS, ITGAE*, ***KIAA1199***, *LEP*, ***LETM2, MEST, MUC13***, *NKX2-1*, ***P4HA1***, phosphatidylinositol, ***PITPNC1***, *PLOD1*, ***PLOD2***, *PML, PRKCZ, PSEN1, PTEN*, ***ROR1, SEMA3B***, *SKI*, ***SPAG4***, talin, *TGFA, TGFB1, VCL, VIP, ZFP36*	18	12	Cancer cell cycle, cellular growth and proliferation
9	*AP2A2*, ***ARSJ***, *CDH23*, ***CEACAM7***, *CTNNB1, EGF, ERBB2IP*, ***FZD8, GPR64***, *GRB2*, ***HIPK2, IDS***, *JAK2*, ***JUP***, *LEF1*, ***MAST4***, *MYO7A*, ***PHACTR2***, *PKD1, PSEN1, PTPRF, RAF1, SKI, SMAD1, SMAD3, SUMF1*, ***SVEP1***, *TCF7L2 (includes EG:6934), TGFA*, ***UBASH3B, USH1C***, *USH1G, VIP, ZFP36, ZFYVE9*	17	12	Genetic disorder, neurologic disease, cellular development

NOTE: After analysis through Ingenuity Pathways, we identified nine main gene networks. Genes affected by silencing of hnRNP A2/B1, focus molecules, are shown in bold italics.

clustered small cells together with foci of bigger cells (Fig. 2). After 96 hours postseeding, A549 siA cells were not fully confluent but showed very compact regions of smaller cells where cells were piling up. Similar results were observed in mesenchymal H1703 cells. Confluent H1703 EV cells did not attach to each other and did not cluster. H1703 siA cells formed clusters of more compact cells with increased cell-cell contact compared with H1703 EV cells (Fig. 2). In contrast, no changes were observed in the epithelial H358 cell line after silencing hnRNP A2/B1 (data not shown).

Silencing hnRNP A2/B1 increases proliferation and colony formation in nonepithelial cell lines

To further investigate hnRNP A2/B1 function in lung cancer cell lines, we evaluated proliferation by cell growth assay (MTS). After 4 days, A549 siA cells showed a significant increase in proliferation compared with A549 EV cells. A similar result was obtained with H1703 siA cells compared with H1703 EV cells (Fig. 3A). Moreover, silencing hnRNP A2/B1 enhanced the ability to form colonies on the anchorage-independent clonogenic assay. A549 siA showed a 794% increase in the number of colonies compared with A549 EV. H1703 siA showed a 174% increase over H1703 EV in the number of colonies counted per field (Fig. 3B). These changes in number of colonies correlated with changes in the size and morphology of the colonies. A549 siA produced bigger colonies than A549 EV (Fig. 3B). H1703 siA formed bigger and more compact colonies than H1703 EV (Fig. 3B). H358 siA cells did not show any differences in growth compared with

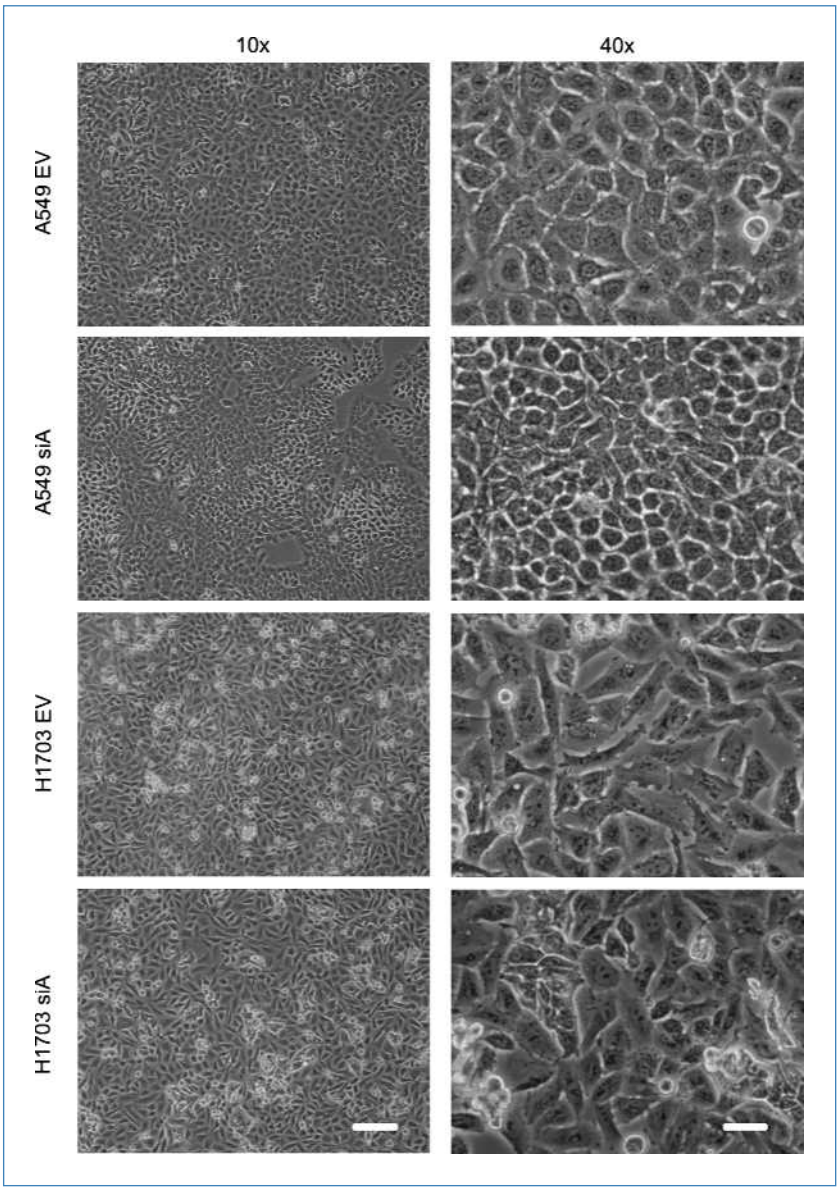

Figure 2. Morphologic changes after silencing hnRNP A2/B1. Cells were seeded at 1 × 10^6 per flask in T75 flask. Images at 10× and 40× magnification. Scale bar at 10×, 40 μm; at 40×, 10 μm.

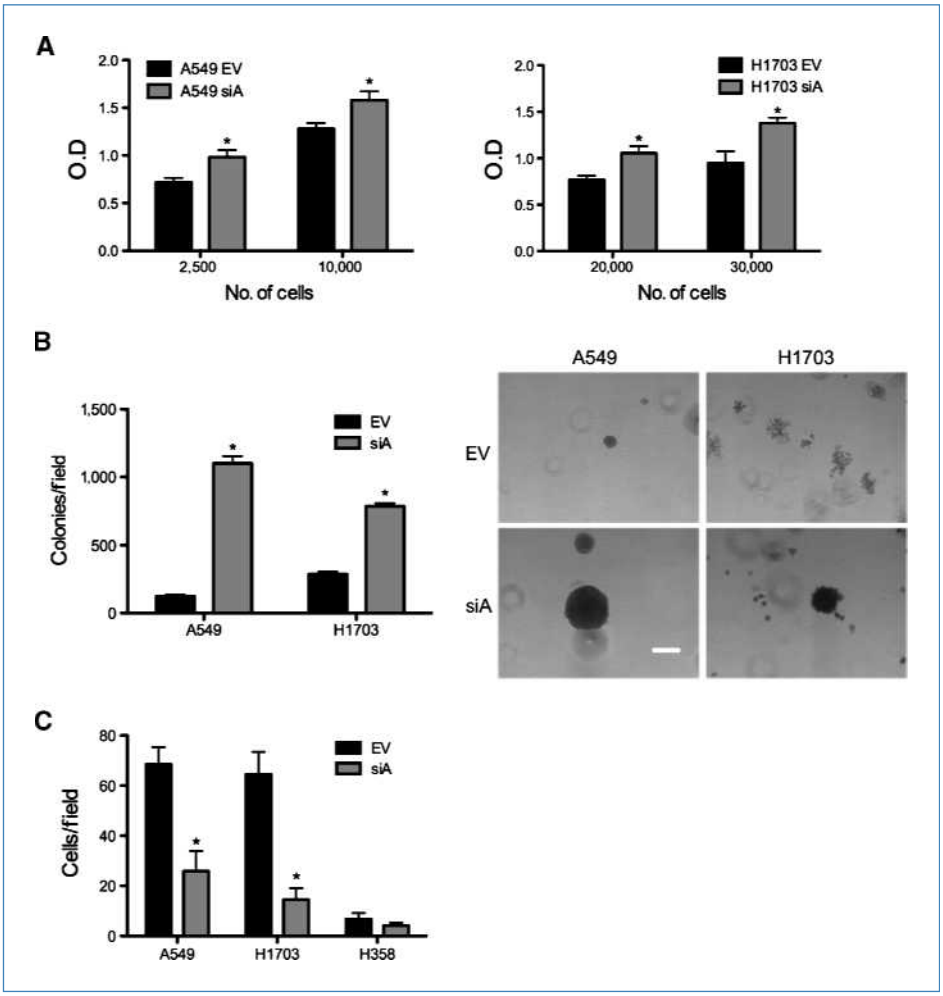

Figure 3. Silencing hnRNP A2/B1 increases proliferation and decreases migration. A, MTS proliferation assay. *, $P < 0.001$, Student's t test. B, anchorage-independent growth assay. Left, average of colonies per field. *, $P < 0.001$, Student's t test. Right, 10× magnification to show differences in colonies after silencing hnRNP A2/B1. C, migration assay. *, $P < 0.001$, Student's t test. All experiments were repeated at least three times. Scale bar, 40 μm.

H358 EV, and both cell lines did not form colonies in clonogenic assay (data not shown).

Silencing hnRNP A2/B1 inhibits migration in lung cancer cell lines

In addition, we evaluated the effect of hnRNP A2/B1 in migration. A549 EV and H1703 EV migration activity was similar, whereas H358 EV showed less migration (Fig. 3C). H1703 siA showed less migration (4.45-fold) compared with H1703 EV. A549 siA showed 2.65-fold less migration compared with A549 EV. H358 siA also exhibited less migration than H358 EV (1.6-fold decrease). Therefore, all cell lines showed a decrease in migration after silencing hnRNP A2/B1, although the effect was only significant in nonepithelial cell lines H1703 and in A549.

hnRNP A2/B1 affects expression of EMT markers in A549 and H1703 cell lines

Microarray analysis showed downregulation of fibronectin, an EMT marker, after silencing hnRNP A2/B1 in A549. We have confirmed downregulation of fibronectin in A549 siA cell line compared with A549 EV (Fig. 4A and B). However, expression of fibronectin in mesenchymal H1703 was very low, and we were not able to detect changes (Fig. 4A). Given the central role of E-cadherin in EMT control, we explored how hnRNP A2/B1 silencing affected E-cadherin expression (28, 29). Although E-cadherin expression was not detected by the microarray analysis, we evaluated changes in E-cadherin expression at the mRNA and protein levels in A549 and H1703 cell lines. We have observed upregulation of E-cadherin expression in A549 siA and H1703 siA cell lines compared with their EV counterparts at the mRNA level (Fig. 4A). Also, we found a modest increase in E-cadherin protein expression in A549 siA and an important increase in H1703 siA compared with H1703 EV (Fig. 4B). Through immunofluorescence, we have shown that E-cadherin expression in A549 EV is present in the membrane. There was also a diffuse staining in the cytoplasm, whereas there was a more abundant E-cadherin signal in the membrane of A549 siA cells along areas of cell-cell contacts. H1703EV cells were negative for E-cadherin expression, but H1703 siA cells showed clusters of E-cadherin–positive cells. In the same field, nonclustered cells without cell-cell contacts were E-cadherin negative (Fig. 4C).

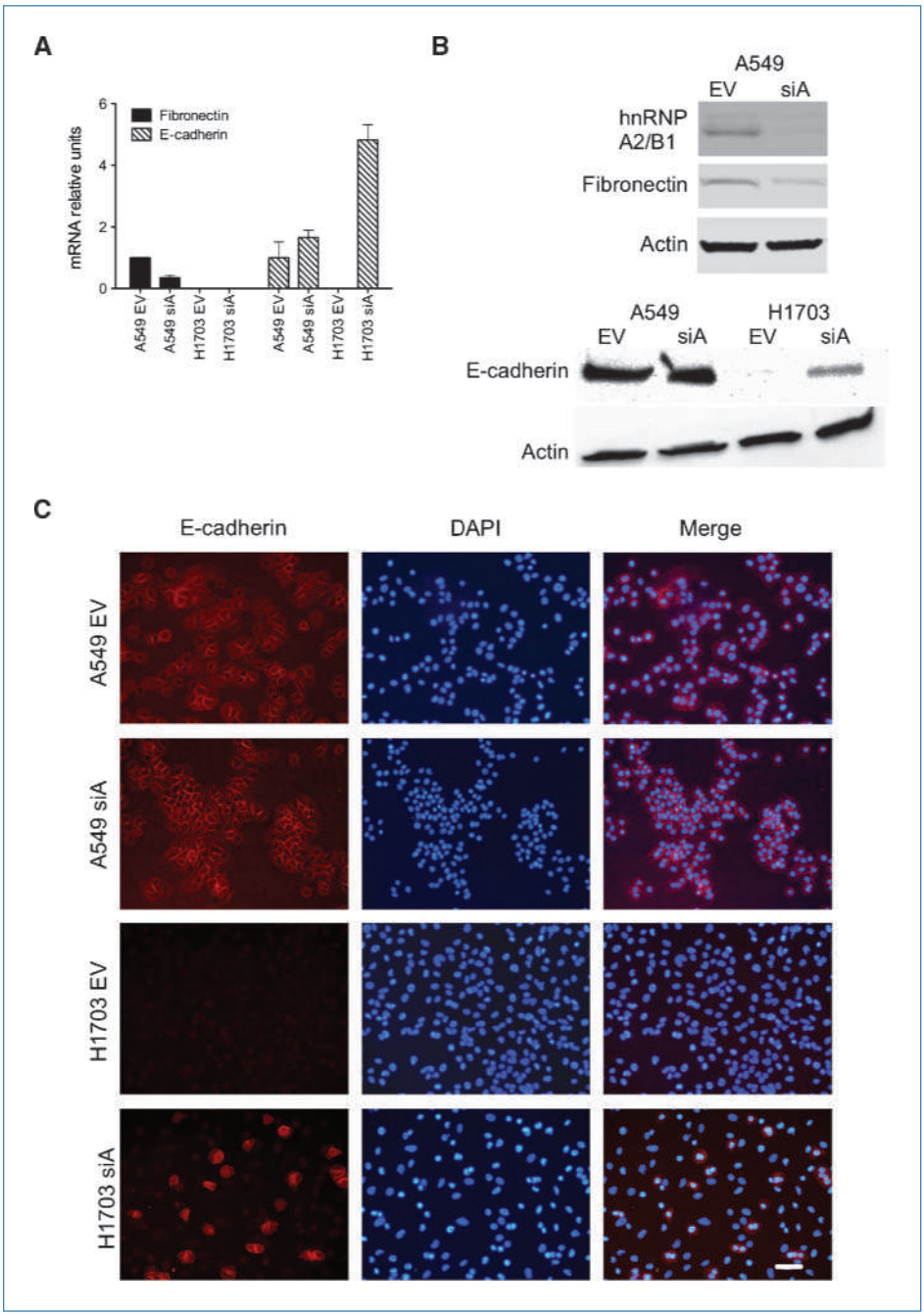

Figure 4. Silencing hnRNP A2/B1 effect on EMT markers. A, real-time PCR for fibronectin and E-cadherin. B, fibronectin and E-cadherin Western blot analysis from whole-cell extracts after 24 hours postseeding. C, E-cadherin immunofluorescence staining. Experiments were repeated three times. Scale bar, 20 μm.

Expression of E-cadherin inhibitors Snai1 and Twist, but not ZEB-1, is affected by silencing hnRNP A2/B1 in nonepithelial cell lines

To further study the effect of hnRNP A2/B1 in modulation of EMT and regulation of E-cadherin expression, we have explored the effect of hnRNP A2/B1 in E-cadherin inhibitors Twist, Snai1, and ZEB-1 (32, 33). We have observed that A549 siA cells showed a higher and constant level of expression of E-cadherin mRNA, whereas A549 EV had lower and downregulated expression of E-cadherin (Fig. 5A). We examined Snai1 expression and found that at 2 hours postseeding, Snai1 mRNA peaked in A549 EV cells. This peak was more attenuated in A549 siA cells. After 4 hours postseeding, Snai1 mRNA was downregulated in both cell lines (Fig. 5B). Snai1 protein expression followed the same pattern but was slightly delayed in time (Fig. 5B). However, H1703 cell line did not show this peak of expression after 2 hours postseeding in Snai1 mRNA expression (data not show). Twist was downregulated in both A549 siA and H1703 siA cells (Fig. 5C). Another E-cadherin inhibitor, ZEB-1, was not affected by

silencing of hnRNP A2/B1 in A549 and H1703 cell lines (data not shown).

To confirm the role of hnRNP A2/B1 in the regulation of E-cadherin and E-cadherin inhibitors, we overexpressed hnRNP A2/B1 in A549 by stable transfection. Overexpression of hnRNP A2/B1 in A549 A2B1rec correlated with an increase of Snai1 and Twist expression. Changes in E-cadherin expression were also observable (Fig. 5D).

Discussion

We and others have reported hnRNP A2/B1 as an early lung cancer marker (11–15). However, despite increasing evidence of a prominent role for hnRNP A2/B1 in the regulation of mRNA processing (1, 2, 4), telomere maintenance (3), cell metabolism (10), migration and invasion (9, 25, 26), proliferation (22–24), and cellular response to mitochondrial stress (26), there is no described mechanistic link for the contribution of hnRNP A2/B1 overexpression and the pathogenesis of lung cancer. To approach this question, we have silenced hnRNP A2/B1 in a panel of lung cancer cell lines that present a different EMT phenotype: mesenchymal H1703, intermediate A549, and epithelial H358 (30). EMT differentiation has been reported to affect migration and proliferation (28, 29), and EMT induction has been observed as part of a response to mitochondrial stress (27).

Results of silencing hnRNP A2/B1 have been reported in a number of human cancer cell lines but not in lung cancer cell lines (22–24). In this study, we have analyzed, for the first time, the effect of silencing hnRNP A2/B1 in lung cancer cell lines. Our results lead to four main observations: (*a*) microarray analysis expression in A549 reveals that silencing of hnRNP A2/B1 alone has a strong effect on genes that are fundamental to several hallmarks of cancer (34). Several affected genes are known to play a role during development and affect motility, migration, and proliferation. (*b*) hnRNP A2/B1 regulates morphology and cell growth in nonepithelial cell lines. Morphologic changes correlate with a different growth pattern.

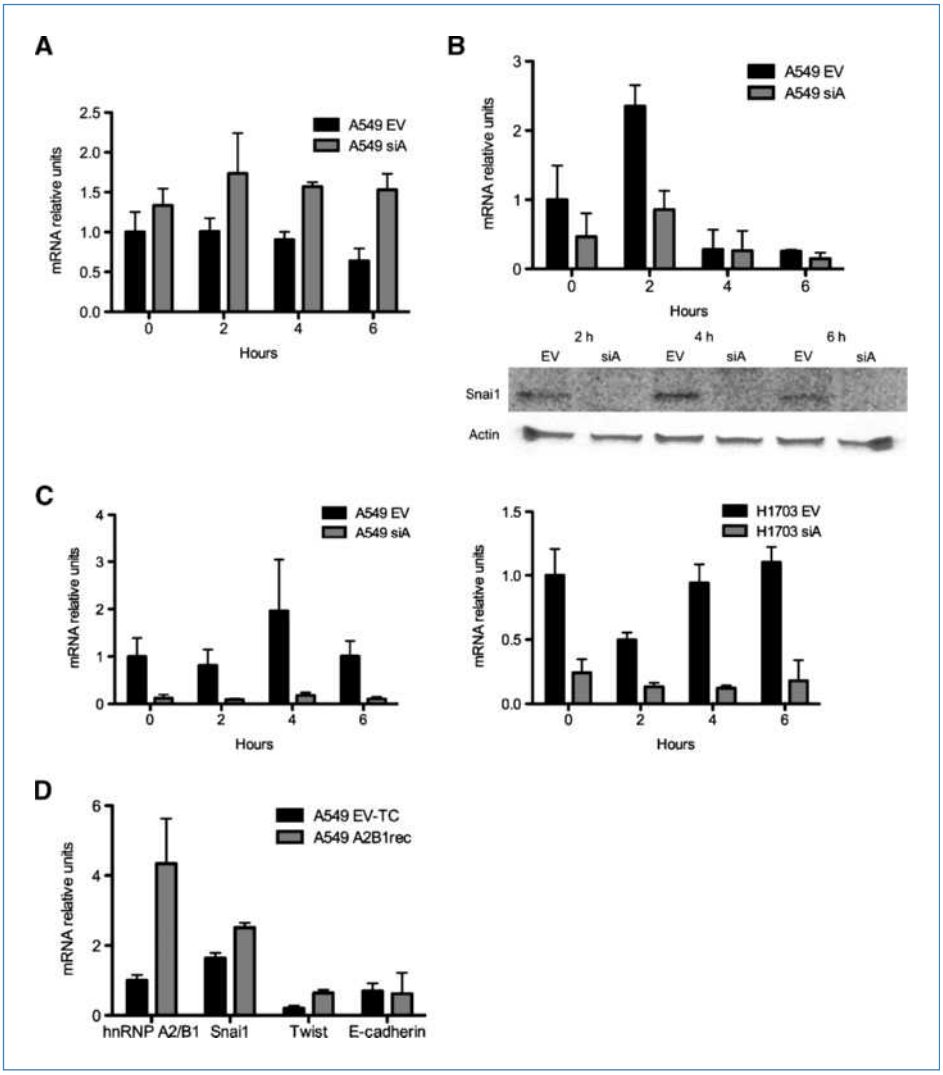

Figure 5. E-cadherin regulation. A, real-time PCR of E-cadherin, A549. B, top, real-time PCR of Snai1, A549. Bottom, Snai1 protein expression in A549. C, real-time PCR for Twist. Left, A549. Right, H1703. D, real-time PCR of Snai1, Twist, and E-cadherin after overexpression of hnRNP A2/B1 in A549. Results are representative of three experiments.

Interestingly, a greater effect in proliferation is observed after silencing hnRNP A2/B1 in an anchorage-independent assay than in a two-dimensional assay. Changes in proliferation take place without inducing changes in hnRNP A1 expression, which contradicts the cooperative hnRNP interaction hypothesis proposed by Patry and colleagues (22). (*c*) Migration is affected by silencing of hnRNP A2/B1. These effects correlate with changes observed in the microarray expression analysis that showed a number of genes involved in cell motility and migration. The effect on migration is present in all cell lines studied but is only statistically significant in nonepithelial cell lines. (*d*) Proliferation and migration changes observed after silencing hnRNP A2/B1 are more relevant in intermediate A549 and in mesenchymal H1703 than in epithelial H358.

All these reported changes, including cell morphology, increased proliferation, decreased migration, together with increase in E-cadherin, decrease of fibronectin, and downregulation of Snai1 and Twist are consistent with transition from a mesenchymal to an epithelial phenotype. Therefore, we propose that silencing hnRNP A2/B1 expression may revert EMT, inducing a mesenchymal-to-epithelial transition (MET) process. Induction of MET after silencing hnRNP A2/B1 in nonepithelial cell lines could be explained by the upregulation of E-cadherin expression as a consequence of Snai1 and Twist downregulation. However, A549 and H1703 show a different pattern of expression of E-cadherin inhibitors although the fact that Twist is downregulated in both cell lines but not Snai1 may indicate a predominant role for Twist in the Twist-Snai1 axis as it has been suggested previously (35). Although previous reports have linked suppression of EMT by silencing Snai1 and/or Twist with decrease in cell proliferation (35, 36), in our study, reversion of EMT increases cell proliferation. This could be explained by the fact that in our microarray, we detected upregulation of ErbB3 and versican (37) and downregulation of TGF-β2, tumor suppressor HIPK2 (38–40), and GDF15 (41).

We have also shown that there is a correlation between cell density and hnRNP A2/B1 expression. Previous reports have indicated that VHL affects hnRNP A2/B1 expression, and VHL is also regulated by cell density (42, 43). According to the reported observations, we suggest a link between cell density, hnRNP A2/B1 expression, and EMT regulation in nonepithelial cancer cells. Tumor cell growth increases cell density and levels of hnRNP A2/B1 protein. Under these conditions, E-cadherin is downregulated, favoring EMT. Detached cells, which may be *in vitro* analogues of metastatic cells at low density, may show low levels of hnRNP A2/B1. This could increase proliferation and upregulation of E-cadherin that would permit cells to attach to a new site. However, epithelial-like cells with high expression of E-cadherin, such as H358, would not be expected to respond to silencing of hnRNP A2/B1 in a significant way. A consequence of this hypothesis is that an increase of hnRNP A2/B1 expression may be regulating EMT. Our results support this possibility because we have shown that overexpression of hnRNP A2/B1 in A549 correlates with an upregulation of Snai1 and Twist expression.

In our results, epithelial H358 cell line was not affected by silencing of hnRNP A2/B1. We suggest that cell lines from previous reports (22–24) may have a different status of EMT-MET differentiation that could explain these different results reported after hnRNP A2/B1 silencing. Alternatively, cell line–specific differences in regulation of hnRNP A2/B1 related to cell density may affect the functional effects observed after silencing hnRNP A2/B1.

The fact that hnRNP A2/B1 has a role in the control of cell metabolism by regulating alternative splicing of M1/M2 pyruvate kynase isozymes (10) may explain the integration of cell density and regulation of hnRNP A2/1 expression. This suggests a complex network of interaction between cell metabolism, cell density, cellular stress, and EMT differentiation in which hnRNP A2/B1 may play a regulatory role. An important consequence of the relationship between cell density and hnRNP A2/B1 expression status is that to obtain consistent experimental results while studying hnRNP A2/B1 function, cell handling, cell density at the time of splitting flasks, and seeding density, all need to be carefully defined and standardized.

In light of our preliminary description of the regulatory influence of hnRNP A2/B1 and its effect on clonogenic growth, cell migration, and proliferation, coupled with other recent reports on hnRNP A2/B1 regulation of core biology, further studies are needed to understand the underlying mechanism of regulation of EMT/MET linked to hnRNP A2/B1 expression and cell density in lung cancer, relative to its contribution to lung carcinogenesis.

Disclosure of Potential Conflicts of Interest

No potential conflicts of interest were disclosed.

Grant Support

This research was supported in part by intramural NCI funds, Rush University, and the Charles J. & Margaret Roberts Fund.

Received 03/10/2010; revised 06/30/2010; accepted 07/14/2010; published OnlineFirst 08/31/2010.

References

1. Krecic AM, Swanson MS. hnRNP complexes: composition, structure, and function. Curr Opin Cell Biol 1999;11:363–71.
2. Dreyfuss G, Kim VN, Kataoka N. Messenger-RNA-binding proteins and the messages they carry. Nat Rev Mol Cell Biol 2002;3:195–205.
3. Moran-Jones K, Wayman L, Kennedy DD, et al. hnRNP A2, a potential ssDNA/RNA molecular adapter at the telomere. Nucleic Acids Res 2005;33:486–96.
4. Cooper TA, Wan L, Dreyfuss G. RNA and disease. Cell 2009;136:777–93.
5. Zhou J, Allred DC, Avis I, et al. Differential expression of the early lung cancer detection marker, heterogeneous nuclear ribonucleoprotein-A2/B1 (hnRNP-A2/B1) in normal breast and neoplastic breast cancer. Breast Cancer Res Treat 2001;66:217–24.
6. Yan-Sanders Y, Hammons GJ, Lyn-Cook BD. Increased expression

of heterogeneous nuclear ribonucleoprotein A2/B1 (hnRNP) in pancreatic tissue from smokers and pancreatic tumor cells. Cancer Lett 2002;183:215–20.
7. Lee CL, Hsiao HH, Lin CW, et al. Strategic shotgun proteomics approach for efficient construction of an expression map of targeted protein families in hepatoma cell lines. Proteomics 2003;3:2472–86.
8. Lee CH, Lum JH, Cheung BP, et al. Identification of the heterogeneous nuclear ribonucleoprotein A2/B1 as the antigen for the gastrointestinal cancer specific monoclonal antibody MG7. Proteomics 2005;5:1160–6.
9. Moran-Jones K, Grindlay J, Jones M, Smith R, Norman JC. hnRNP A2 regulates alternative mRNA splicing of TP53INP2 to control invasive cell migration. Cancer Res 2009;69:9219–27.
10. Clower CV, Chatterjee D, Wang Z, Cantley LC, Vander Heiden MG, Krainer AR. The alternative splicing repressors hnRNP A1/A2 and PTB influence pyruvate kinase isoform expression and cell metabolism. Proc Natl Acad Sci U S A 2010;107:1894–9.
11. Zhou J, Mulshine JL, Unsworth EJ, et al. Purification and characterization of a protein that permits early detection of lung cancer. Identification of heterogeneous nuclear ribonucleoprotein-A2/B1 as the antigen for monoclonal antibody 703D4. J Biol Chem 1996;271:10760–6.
12. Tockman MS, Mulshine JL, Piantadosi S, et al. Prospective detection of preclinical lung cancer: results from two studies of heterogeneous nuclear ribonucleoprotein A2/B1 overexpression. Clin Cancer Res 1997;3:2237–46.
13. Zhou J, Mulshine JL, Ro JY, et al. Expression of heterogeneous nuclear ribonucleoprotein A2/B1 in bronchial epithelium of chronic smokers. Clin Cancer Res 1998;4:1631–40.
14. Fielding P, Turnbull L, Prime W, Walshaw M, Field JK. Heterogeneous nuclear ribonucleoprotein A2/B1 up-regulation in bronchial lavage specimens: a clinical marker of early lung cancer detection. Clin Cancer Res 1999;5:4048–52.
15. Zhou J, Nong L, Wloch M, Cantor A, Mulshine JL, Tockman MS. Expression of early lung cancer detection marker: hnRNP-A2/B1 and its relation to microsatellite alteration in non-small cell lung cancer. Lung Cancer 2001;34:341–50.
16. Tockman MS, Gupta PK, Myers JD, et al. Sensitive and specific monoclonal antibody recognition of human lung cancer antigen on preserved sputum cells: a new approach to early lung cancer detection. J Clin Oncol 1988;6:1685–93.
17. Man YG, Martinez A, Avis IM, et al. Phenotypically different cells with heterogeneous nuclear ribonucleoprotein A2/B1 overexpression show similar genetic alterations. Am J Respir Cell Mol Biol 2000; 23:636–45.
18. Pino I, Pio R, Toledo G, et al. Altered patterns of expression of members of the heterogeneous nuclear ribonucleoprotein (hnRNP) family in lung cancer. Lung Cancer 2003;41:131–43.
19. Hilbe W, Dirnhofer S, Greil R, Woll E. Biomarkers in non-small cell lung cancer prevention. Eur J Cancer Prev 2004;13:425–36.
20. Montuenga LM, Zhou J, Avis I, et al. Expression of heterogeneous nuclear ribonucleoprotein A2/B1 changes with critical stages of mammalian lung development. Am J Respir Cell Mol Biol 1998;19:554–62.
21. Peebles KA, Dwyer-Nield LD, Malkinson AM. Altered expression of splicing factor, heterogeneous nuclear ribonucleoprotein A2/B1, in mouse lung neoplasia. Mol Carcinog 2007;46:887–900.
22. Patry C, Bouchard L, Labrecque P, et al. Small interfering RNA-mediated reduction in heterogeneous nuclear ribonucleoparticule A1/A2 proteins induces apoptosis in human cancer cells but not in normal mortal cell lines. Cancer Res 2003;63:7679–88.
23. He Y, Brown MA, Rothnagel JA, Saunders NA, Smith R. Roles of heterogeneous nuclear ribonucleoproteins A and B in cell proliferation. J Cell Sci 2005;118:3173–83.
24. He Y, Rothnagel JA, Epis MR, Leedman PJ, Smith R. Downstream targets of heterogeneous nuclear ribonucleoprotein A2 mediate cell proliferation. Mol Carcinog 2009;48:167–79.
25. Pan H, Luo C, Li R, et al. Cyclophilin A is required for CXCR4-mediated nuclear export of heterogeneous nuclear ribonucleoprotein A2, activation and nuclear translocation of ERK1/2, and chemotactic cell migration. J Biol Chem 2008;283:623–37.
26. Guha M, Pan H, Fang JK, Avadhani NG. Heterogeneous nuclear ribonucleoprotein A2 is a common transcriptional coactivator in the nuclear transcription response to mitochondrial respiratory stress. Mol Biol Cell 2009;20:4107–19.
27. Naito A, Cook CC, Mizumachi T, et al. Progressive tumor features accompany epithelial-mesenchymal transition induced in mitochondrial DNA-depleted cells. Cancer Sci 2008;99:1584–8.
28. Thiery JP, Sleeman JP. Complex networks orchestrate epithelial-mesenchymal transitions. Nat Rev Mol Cell Biol 2006;7:131–42.
29. Thiery JP. Epithelial-mesenchymal transitions in tumour progression. Nat Rev Cancer 2002;2:442–54.
30. Thomson S, Buck E, Petti F, et al. Epithelial to mesenchymal transition is a determinant of sensitivity of non-small-cell lung carcinoma cell lines and xenografts to epidermal growth factor receptor inhibition. Cancer Res 2005;65:9455–62.
31. Rasband WS. ImageJ, U.S. National Institutes of Health, Bethesda (MD); c1997-2009. Available from: http://rsb.info.nih.gov/ij/.
32. Kalluri R, Weinberg RA. The basics of epithelial-mesenchymal transition. J Clin Invest 2009;119:1420–8.
33. Zeisberg M, Neilson EG. Biomarkers for epithelial-mesenchymal transitions. J Clin Invest 2009;119:1429–37.
34. Hanahan D, Weinberg RA. The hallmarks of cancer. Cell 2000;100: 57–70.
35. Smit MA, Geiger TR, Song JY, Gitelman I, Peeper DS. A Twist-Snail axis critical for TrkB-induced epithelial-mesenchymal transition-like transformation, anoikis resistance, and metastasis. Mol Cell Biol 2009;29:3722–37.
36. Olmeda D, Jorda M, Peinado H, Fabra A, Cano A. Snail silencing effectively suppresses tumour growth and invasiveness. Oncogene 2007;26:1862–74.
37. Sheng W, Wang G, La Pierre DP, et al. Versican mediates mesenchymal-epithelial transition. Mol Biol Cell 2006;17:2009–20.
38. D'Orazi G, Cecchinelli B, Bruno T, et al. Homeodomain-interacting protein kinase-2 phosphorylates p53 at Ser 46 and mediates apoptosis. Nat Cell Biol 2002;4:11–9.
39. Di Stefano V, Blandino G, Sacchi A, Soddu S, D'Orazi G. HIPK2 neutralizes MDM2 inhibition rescuing p53 transcriptional activity and apoptotic function. Oncogene 2004;23:5185–92.
40. Puca R, Nardinocchi L, Gal H, et al. Reversible dysfunction of wild-type p53 following homeodomain-interacting protein kinase-2 knockdown. Cancer Res 2008;68:3707–14.
41. Bauskin AR, Brown DA, Kuffner T, et al. Role of macrophage inhibitory cytokine-1 in tumorigenesis and diagnosis of cancer. Cancer Res 2006;66:4983–6.
42. Pioli PA, Rigby WF. The von Hippel-Lindau protein interacts with heteronuclear ribonucleoprotein a2 and regulates its expression. J Biol Chem 2001;276:40346–52.
43. Mohan S, Burk RD. von Hippel-Lindau protein complex is regulated by cell density. Oncogene 2003;22:5270–80.